

Influence of chain structure on the crystallization mechanism of poly(vinylidene fluoride)/poly(methyl acrylate) blends: evidence of chain extension due to blending

Pralay Maiti and Arun K. Nandi*

Polymer Science Unit, Indian Association for the Cultivation of Science, Jadavpur, Calcutta 700 032, India

(Received 14 August 1996; revised 17 March 1997)

The head to head (H–H) defect structure of poly(vinylidene fluoride) (PVF₂) has a dramatic effect on the crystallization rate of PVF₂ and its blends. At a fixed temperature the crystallization rate decreases with increase in H–H defect and also with increase in the concentration of amorphous polymer, poly(methyl acrylate) (PMA), in the blend. But under the same degree of supercooling the crystallization rate of PVF₂ increases with increase in H–H defect concentration. The molecular mechanism of crystallization of PVF₂ is very much dependent on the H–H defect structure present in the chains. Analysis by the Lauritzen and Hoffman (L–H) equation of crystallization rate indicates a regime I–regime II break for lower defect content (3.75%) PVF₂ fraction and a regime II–regime III break for higher defect content (5% and 5.6%) PVF₂ fractions. However, analysis of the kinetic data of PVF₂ blends by the modified L–H equation indicates only the regime II → III break irrespective of the H–H defect present in the PVF₂ samples. The regime transition temperature is dependent on both the H–H defect concentration and also on the PMA concentration in the blend. The chain extension factor (α), calculated from the ratio of the lateral surface energy (σ) values of pure polymer and that of blends, have values greater than unity for almost all cases. © 1997 Elsevier Science Ltd.

(Keywords: crystallization rate; polymer blends; regime transition)

INTRODUCTION

There is a dramatic reduction of crystallization rate of the crystalline polymer in its miscible blends with amorphous polymers^{1–5}. The crystallization mechanisms in these polymer blends are different from those of the unblended systems^{1–3}. In the melt of the blend the amorphous polymer should diffuse away from the crystal growth front. So, the crystallization rate is influenced not only by the initial composition of the melt but also by the local changes of the composition due to such depletion. This builds up a depletion layer at the interface and it also contains the low molecular weight fraction and structurally irregular fraction of the crystalline polymer⁶. This depleted layer affects the crystallization rate in two ways: (i) the transport of the crystallisable units to the growth front becomes affected, and (ii) the nucleation rate is also reduced due to the depression of the equilibrium melting point at this zone. The composition of the melt at the growth front is dependent on the diffusion coefficient, initial composition of the melt and also on the growth rate. Therefore, in the compatible blends it is very difficult to achieve a correct expression of crystallization rate covering all these factors⁶.

The crystallization of unblended polymers are usually explained by the Lauritzen–Hoffman (L–H) growth rate theory⁷. However, Wang and Nishi¹ explained the crystallization rates of the blends by applying the above theory taking the T_g and T_m^0 values of the blends. Some workers

modified the L–H growth rate equation by introducing the concentration of crystallizing units in the equation^{3,4}. More meaningful approaches to analyze the crystallization rate in these blends have been made by Ong and Price² and Alfonso and Russel⁵ by considering the dilution effect on the free energy of formation (ΔF^*) of the critical size nucleus. The former authors used the model of Boon and Azcue⁸ while the latter group used the lattice model of Flory⁹ and Mandelkern¹⁰ for the ΔF^* in the presence of a polymer–diluent system.

In this paper we have analyzed the crystallization kinetics data for the blends of PVF₂ fractions with PMA based on the extended form of L–H growth rate theory⁸ applicable to the polymer blends²:

$$G = G_0 \phi_2 \exp \left[\frac{-U^*}{R(T - T_\alpha)} \right] \exp \left[\frac{-K_g(i)}{T(T_{mb}^0 - T)} + \frac{0.2T_m^0 \ln \phi_2}{T_{mb}^0 - T} \right] \quad (1)$$

where G is the crystal growth rate, G_0 the pre-exponential factor, ϕ_2 the volume fraction of the crystalline polymer, U^* the activation energy of transport, $T_\alpha = (T_g - 30)$ K, T is the temperature of crystallization, T_{mb}^0 is the equilibrium melting point of the crystal in the blend, $K_g(i)$ is the nucleation constant of the i th regime: $K_g(I) = 2K_g(II) = K_g(III)$ with $K_g(I) = 4b\sigma\sigma_e T_{mb}^0 / k\Delta h_f$ where σ , σ_e are the lateral and end surface free energies, respectively, b is the thickness of the nucleus, k is the Boltzmann constant and Δh_f is the enthalpy of fusion per unit volume. The first exponential term indicates the contribution of transport process in the crystallization rate and the second exponential term indicates the

* To whom correspondence should be addressed

contribution of the nucleation process in the crystallization rate. The pre-exponential factor is multiplied by ϕ_2 because the nucleation rate is proportional to the concentration of crystallisable units¹¹.

The lateral surface free energy (σ) of the polymer crystal can be determined from the analysis of crystallization kinetics, provided the end surface free energy (σ_e) is known¹². Recently, Hoffman *et al.*¹³ related the lateral surface free energy (σ) of a polymer crystal with the chain configuration parameter, the characteristic ratio (c_α), in the pure melt of the polymer by the relation

$$\sigma = \Delta H_f(a/2) \frac{1}{c_\alpha} \quad (2)$$

where ΔH_f is the enthalpy of fusion (erg cm⁻³), a is the width of the chain and

$$C_\alpha = \frac{\bar{r}_o^2}{nl^2} \quad (3)$$

\bar{r}_o^2 is the mean square end to end distance in the unperturbed state, l is the diameter of the segment and n is the number of segments in the chain¹⁴. Polymer chains adopt the unperturbed dimension in an unblended melt, but may be extended by a factor α in the blended condition due to their interaction with the chain of other polymer. Extending the above relation to the case of blends¹⁵

$$\sigma_b = \Delta H_f(a/2) \frac{1}{C_\alpha}$$

where C_α assumes a value $(\alpha \bar{r}_o^2)/(nl^2)$.

One can calculate α for different compositions of the blend from the relation

$$\alpha = (\sigma/\sigma_b)^{1/2} \quad (4)$$

Thus measuring the surface free energies of the crystal both from unblended polymer and also from its blended state, one can calculate the molecular extension factor.

Poly(vinylidene fluoride) (PVF₂) is not completely isoregic but has a certain amount of head to head (H-H) defect structure¹⁶. The amount of H-H defect structure is dependent on the polymerization condition¹⁷. In the literature, though, some crystallization kinetics of PVF₂¹⁸⁻²¹ and its blends^{1,3,4} are reported but there is yet no report relating the crystallization mechanism of PVF₂ with the head to head (H-H) defect structure present in the chain. In this paper we report the crystallization kinetics of three sharp PVF₂ fractions and their blends with poly(methyl acrylate) (PMA) with special emphasis to their H-H defect structure present in the chain. The chain extension factor (α) measured from the σ values obtained by crystallization kinetics studies will also be presented in this paper.

EXPERIMENTAL

Three sharp PVF₂ fractions (KFE, KYA and KYD) were used in this work. They were obtained from fractional crystallization of KF-1000 (Kureha Chemical Co., Japan) and KY-201 (Pennwalt Corporation, USA) and were characterized using a procedure published earlier²². The fractions were chosen in such a way that the influence of molecular weight on crystallization kinetics can be minimized (KFE and KYA as one pair, KYA and KYD as another pair). The poly(methyl acrylate) (PMA) was fractionated by a liquid-liquid phase separation technique using a benzene/methanol system. The second fraction

Table 1 Characteristics of the samples used

Sample	$\bar{M}_w \times 10^{-5}$	PDI	H-H defect (mol.%)	Crystallinity ^a	M.Pt. ^a (°C)
KFE	5.08	1.43	3.75	53.4	175.0
KYA	6.50	1.77	5.06	49.0	165.2
KYD	7.46	2.45	5.64	46.2	161.6
PMA2	4.04	1.56	—	—	—

^a All the samples were crystallized at 144°C for 24 h.

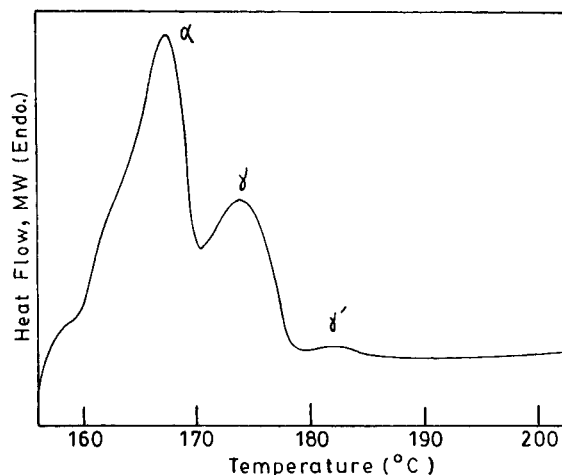


Figure 1 A representative DSC thermogram of the KYA PVF₂ fraction (crystallized at 156°C for 14 h) showing α , γ and γ' phases of PVF₂

(PMA2) was blended with PVF₂ fractions in different compositions using a procedure published earlier²³. The characteristics of the samples are presented in Table 1.

The crystallization kinetics of the systems has been studied using a differential scanning calorimeter (DSC 7, Perkin Elmer) equipped with a 3700 data station. The samples were initially melted at 227°C for 5 min to destroy all the nuclei^{24,25} and then quenched at the rate of 200 deg min⁻¹ to the predetermined isothermal crystallization temperature. Crystallizations were performed for different times at a particular temperature and melted at the heating rate of 10 deg min⁻¹ from the isothermal crystallization temperature to 227°C without cooling. From the endothermic area, crystallinities were calculated taking the enthalpy of fusion per repeating unit ($\Delta H_u^0 = 104.5$ J g⁻¹²⁶). The experiment was repeated for other isothermal crystallization temperatures and in every case the instrument was calibrated with indium before use. During the isothermal crystallization, PVF₂ can crystallize in three different polymorphs α , γ and γ' . Usually, low crystallization temperatures (T_c) and crystallization for smaller times produce the α phase of PVF₂, whereas γ and γ' phases are produced at higher T_c values and also for longer times of crystallization²⁷. The three polymorphs α , γ and γ' are identified in order of increasing melting points in the thermograms²⁸. A representative thermogram showing the melting of the three polymorphs is shown in Figure 1. In the crystallization isotherms, the three phases have been marked wherever they are produced. The equilibrium melting points required for the analysis of the kinetic data have been taken from Ref. 27.

RESULTS AND DISCUSSION

Figures 2–4 show the crystallization isotherms at the indicated temperatures of PVF₂ fractions and their blends of

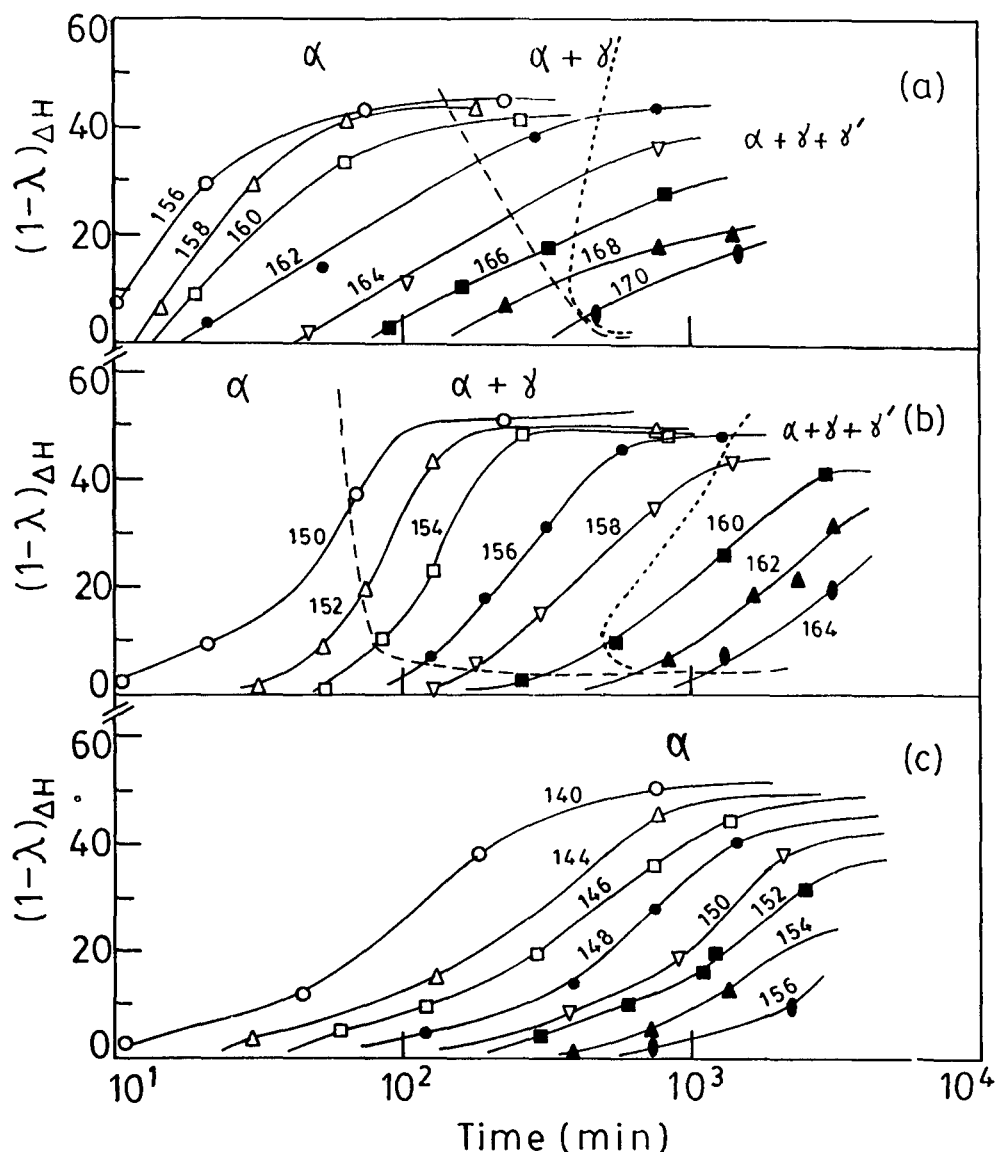


Figure 2 Plots of degree of crystallinity $(1 - \lambda)\Delta H$ versus log time (min) for KFE PVF₂ and its blends with PMA2 at the indicated temperatures (°C): (a) pure KFE, (b) $w_{\text{KFE}} = 0.75$, (c) $w_{\text{KFE}} = 0.47$

compositions (weight fraction) $w_{\text{PVF}_2} = 0.75$ and 0.50 . PVF₂ crystallizes from the melt in three different polymorphs (α , γ and γ') depending on the temperature and time of crystallization²⁸. At the lower crystallization temperature and at lower crystallization times, only the α phase is obtained for all the fractions; γ and γ' phases have been observed at higher T_c values²⁷. This has been denoted by demarcation lines at each figure in a qualitative way. The γ and γ' phases are less abundant with increasing blend composition for each fraction and γ' phases also decrease with increasing H-H defect concentration. Like the crystallization isotherms of other polymers, the crystallization rate exhibits an autocatalytic nature and at the tail part of the isotherms there is retardation in the crystallization rate¹¹.

From Figures 2–4 we first analyze the temperature range (TR) required for the isothermal crystallization within a definite workable time period (1 decade to 3 decades) for different H-H defect content fractions and their blends. The dependency of TR with composition for each PVF₂ fractions has been shown in Figure 5. From the figure it is clear that with increasing PMA concentration in the blend the TR becomes situated progressively at lower

temperatures and this is also true for the PVF₂ fractions and their blends with increasing H-H defect concentration. This indicates that at a given temperature the lower defect content fractions can be crystallized more easily than the higher defect content samples and it is also true for their blends at identical compositions. For each fraction the TR becomes widened with increasing PMA concentration in the blends and this is very much apparent from the Figures 2–4 where the isotherms become gradually closer with increasing blend composition. The reason may lie within the nucleation and growth mechanism of the blend and will be discussed later.

To work out the influence of blend composition on the crystallization rate, plots have been made for $1/\tau_{0.10}$ ($\tau_{0.10}$ = time (min) required to obtain 10% crystallinity) with weight fraction of PMA (w_{PMA}) at a given temperature and are shown in Figure 6a and b. At 156°C there is a sudden drop of crystallization rate of KFE PVF₂ with increasing blend composition and thereafter the decrease is gradual. With increasing T_c the drop of crystallization rate of pure PVF₂ and its blends is gradually lowered for both the KFE and KYA systems. A linear decrease of crystallization rate with

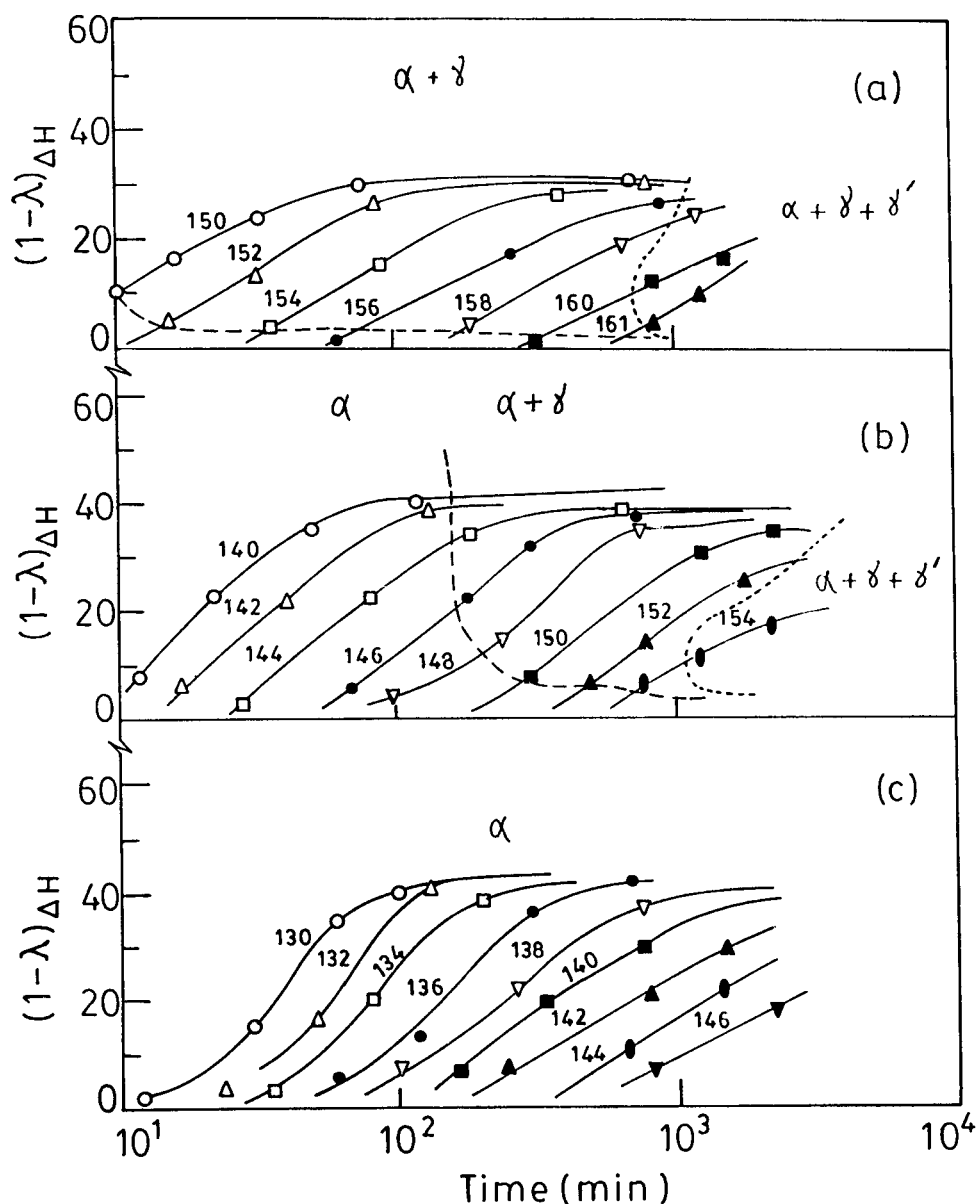


Figure 3 Plots of degree of crystallinity $(1 - \lambda)\Delta H$ versus log time (min) for KYA PVF₂ and its blends with PMA2 at the indicated temperatures (°C): (a) pure KYA, (b) $w_{\text{KYA}} = 0.73$, (c) $w_{\text{KYA}} = 0.48$

composition is expected from equation (1) but the reason for the sudden drop of crystallization rate, particularly at lower isothermal T_c values and at lower PMA concentration in the blend, is unknown. Also, from the figures it is apparent that at a particular temperature (156° or 150°C) the lower defect content fractions and their blends crystallize at a faster rate than the higher defect content samples. This is similar to the behaviour of pure PVF₂ fractions²¹, and the reason is that the higher H–H defect content PVF₂ experiences lesser supercooling than those of lower H–H defect content PVF₂ fractions because the equilibrium melting points of PVF₂ samples decrease with increasing H–H defect content²².

Since the equilibrium melting points of PVF₂ and their blends depend on both the H–H defect concentration as well as on the blend composition^{22,27}, a comparison of the crystallization rate should be made on the basis of the same degree of supercooling to obtain correct thermodynamic information. In Figure 7, the crystallization rate ($\tau_{0.10}^{-1}$) has been plotted with blend composition at $\Delta T(\text{supercooling}) = 40^\circ\text{C}$. It is clear from this figure that there is a slight decrease

of the crystallization rate with composition for KFE PVF₂ but for KYA and KYD PVF₂ fractions the crystallization rate at first decreases faster with increasing w_{PMA} , and at $w_{\text{PMA}} = 0.4$ the rate is same with KFE PVF₂ blends. The slight decrease of crystallization rate of KFE PVF₂ with blend composition at the same supercooling is due to the decrease of ϕ_2 in equation (1). The transport term has not much influence on the crystallization rate in this system because the T_g of the blends (-39°C to -18°C)²⁹ [T_g of PMA = 10°C ³⁰, T_g of PVF₂ = 39°C ³¹] are much lower than the isothermal crystallization temperatures (170–140°C). The cause of initial decrease of crystallization rate with blend composition for KYA and KYD PVF₂ blend may be ascertained from the following discussion. It is clear from the figure that under the same degree of supercooling the higher H–H defect content PVF₂ fractions crystallize at higher rate than that of lower defect content PVF₂ fractions²¹, but this is an abnormal situation because under the same thermodynamic condition the higher defect content material should crystallize slower than the

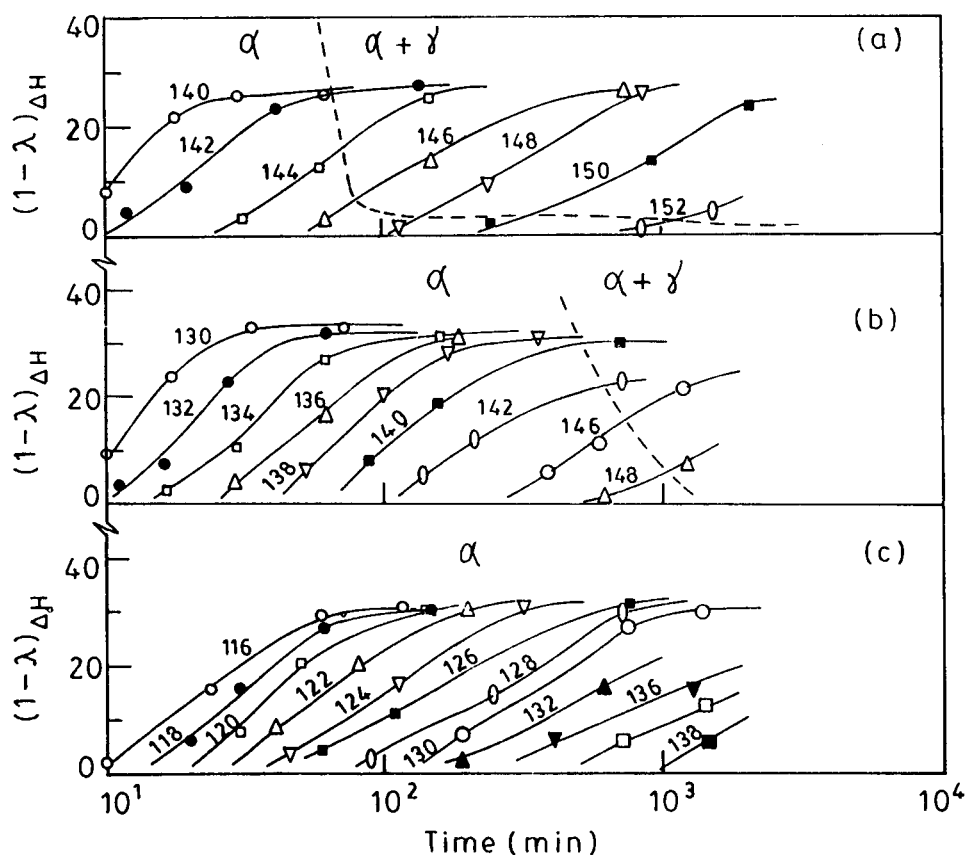


Figure 4 Plots of degree of crystallinity $(1 - \lambda)\Delta H$ versus log time (min) for KYD PVF₂ and its blends with PMA2 at the indicated temperatures (°C): (a) pure KYD, (b) $w_{KYD} = 0.74$, (c) $w_{KYD} = 0.48$

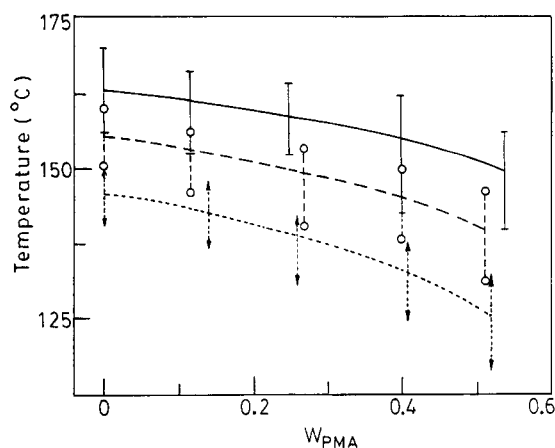


Figure 5 Plots of isothermal crystallization temperature range versus w_{PMA2} : —, KFE; -○-, KYA; ·····, KYD

lower defect content material because of the defect energy. This anomaly can be explained from the fact that in PVF₂ crystal some H-H defects become introduced into the crystal on an equilibrium basis and the higher the concentration of H-H defect in the chain the larger is the amount of defect in the crystal²². These H-H defect content crystals have lower equilibrium melting points than those calculated from Flory's exclusion model^{9,32} of copolymer crystallization. So the depression in T_m^0 is proportional to the amount of H-H defect present in the chain and, therefore, the supercooling calculated from these T_m^0 values does not represent the ideal situation. This is the probable cause for the abnormal behaviour of crystallization of PVF₂ with H-H defect from the pure melt at the same supercooling.

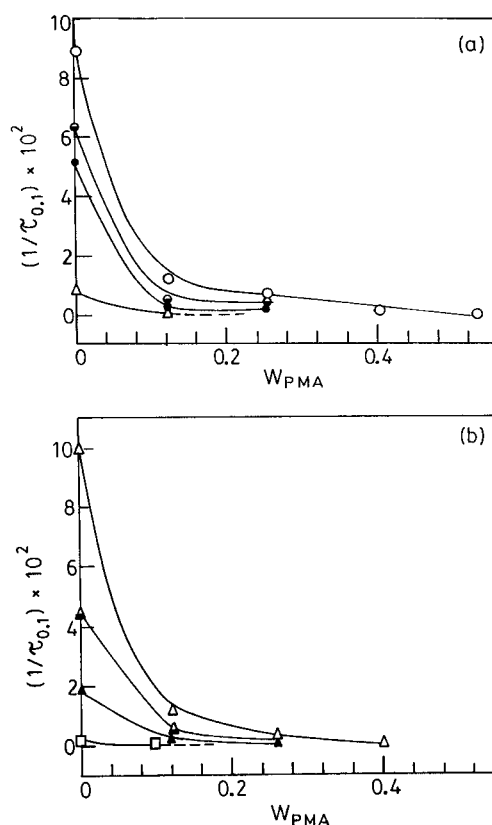


Figure 6 Plots of crystallization rate $(1/\tau_{0.1})$ versus w_{PMA2} : (a) ○, KFE at 156°C; △, KYA at 156°C; ●, KFE at 158°C; ●, KFE at 160°C; (b) △, KYA at 150°C; □, KYD at 150°C; ▲, KYA at 152°C; ▲, KYA at 154°C

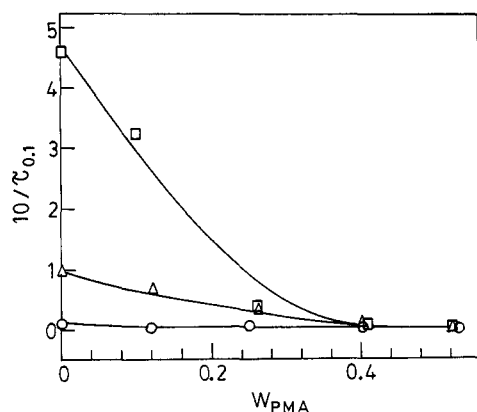


Figure 7 Plot of crystallization rate ($\tau_{0.1}^{-1}$) versus w_{PMA2} at $\Delta T = 40^\circ\text{C}$: \circ , KFE; Δ , KYA; \square , KYD systems

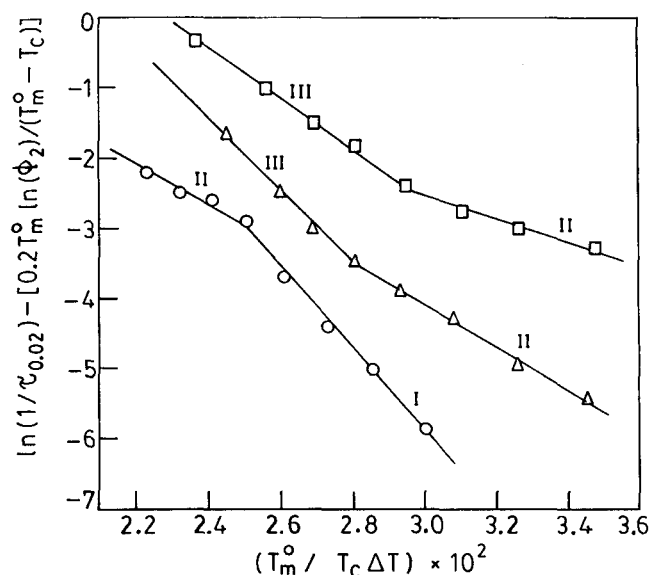


Figure 8 Plot of $\ln(\tau_{0.02}^{-1}) - [0.2T_{mb}^0 \ln(\phi_2)/(T_{mb}^0 - T)]$ versus $T_{mb}^0/\Delta T$ for KFE/PMA2 blends: \circ , $w_{PVF_2} = 1.0$; Δ , $w_{PVF_2} = 0.75$; \square , $w_{PVF_2} = 0.47$

However, it is apparent from the *Figure 7* that, with increasing PMA concentration in KYA and KYD PVF₂ blends, the abnormality is gradually lowered and it is negligible at $w_{PMA} \geq 0.4$. The reason is not yet clear to us and may be due to some fractionation of H-H defect entering into the lamella of higher defect content PVF₂ fractions in the blends.

The crystallization rate will now be analyzed according to equation (1). However, in this system there is a complication in analysing the overall kinetics data because PVF₂ crystallizes in α and γ polymorphs by nucleation and the γ' polymorph is produced by solid state transformation from α polymorph. But until now there has been no nucleation theory presented for the twin polymorph formation from the melt. However, it is clear from *Figures 2–4* that γ and γ' phases are produced at high conversion of melt into the crystal. So by making an approximation that the usual growth rate theory can be applied for the α phase of PVF₂ where the γ and γ' phases are absent, we have analyzed the data according to equation (1)²¹. We have considered the inverse of time required to attain 2% crystallinity ($\tau_{0.02}^{-1}$) as the crystallization rate of the α phase from the melt at different crystallization temperatures. Another approximation has been made in analysing the crystallization rate data

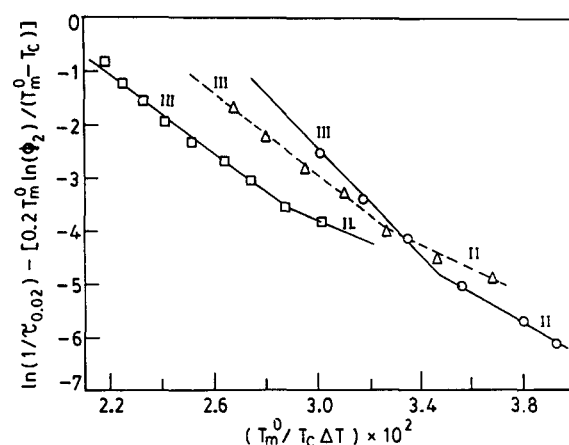


Figure 9 Plot of $\ln(\tau_{0.02}^{-1}) - [0.2T_{mb}^0 \ln(\phi_2)/(T_{mb}^0 - T)]$ versus $T_{mb}^0/\Delta T$ for KYA/PMA2 blends: \circ , $w_{PVF_2} = 1.0$; Δ , $w_{PVF_2} = 0.73$; \square , $w_{PVF_2} = 0.48$

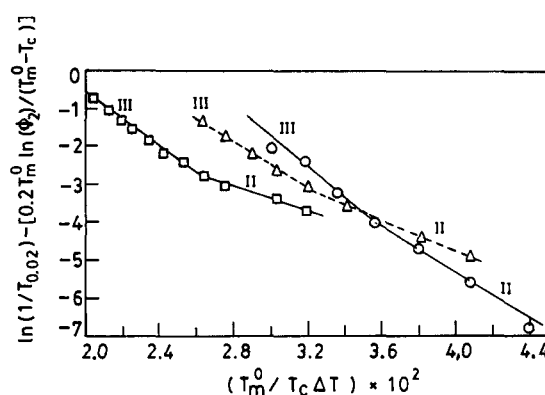


Figure 10 Plot of $\ln(\tau_{0.02}^{-1}) - [0.2T_{mb}^0 \ln(\phi_2)/(T_{mb}^0 - T)]$ versus $T_{mb}^0/\Delta T$ for KYD/PMA2 blends: \circ , $w_{PVF_2} = 1.0$; Δ , $w_{PVF_2} = 0.74$; \square , $w_{PVF_2} = 0.48$

in that the contribution of the transport term in the equation has been considered negligible, because the isothermal crystallization temperatures are much higher ($115\text{--}170^\circ\text{C}$) than the T_g (-39°C to $+18^\circ\text{C}$) for the above compositions of the blend²⁹. Thus, from equation (1) we can plot $\ln(1/\tau_{0.02}) - 0.2T_{mb}^0 \ln(\phi_2)/(T_{mb}^0 - T)$ versus the temperature function $T_{mb}^0/\Delta T$ and the plot may be a straight line or a combination of two intersecting straight lines depending upon the K_g values and hence the regime of crystallization. In *Figures 8–10* the plots are shown for PVF₂ and its blends and from these figures some interesting observations may be made. In *Figure 8*, two intersecting straight lines represent the data very well, but there is a difference in the nature of the two intersecting straight lines of pure KFE and the blends. The pure PVF₂ exhibits a regime I \rightarrow II break¹² while the blends exhibit a regime III \rightarrow II break. A similar change in the regime break of PVF₂ (KF-1000, defect = 3.5%, unfractionated) and its blends with PMA was also observed from growth rate measurements³³ of α spherulites. The reason for such a different behaviour in this blend will be discussed later. In *Figures 9 and 10* KYA and KYD PVF₂ and their blends exhibit the regime break of a similar nature, e.g. a regime III \rightarrow II transition³⁴. From these results it can be concluded that the regime transition in the unblended PVF₂ is dependent on the H-H defect content present in the chain and that in the blends the regime transition is independent of H-H defect content of PVF₂ or on the blend composition.

At this point it is necessary to compare these results with those reported in the literature for pure PVF₂. Nandi and Mandelkern²¹ observed a regime I → II break for lower defect content PVF₂ fraction (H–H defect = 3.36%), a regime I → II → III transition for medium defect content (4.02 and 4.1%) PVF₂ fractions and a regime II → III break for higher defect content (4.99 and 5.54%) PVF₂ fraction. They also analyzed the growth rate data of previous workers^{35,36} with their T_m^0 values²² and observed a regime I → II break for lower (3.81%) defect content Kureha PVF₂ and a regime II → III transition for higher defect content (5.0 and 5.7% H–H defect) Kynar PVF₂ samples. Thus the present data of pure PVF₂ fractions are in good agreement with those of previous workers. Recently, Inoue and coworkers made extensive studies on crystallization rates of PVF₂/poly(methyl methacrylate) (PMMA) blends by optical microscopy³ and by small angle light scattering experiments³⁷. But their results on regime transition of pure PVF₂ sample is contradictory to each other and varies from method to method^{3,37}.

In Table 2 the regime transition temperatures and the supercooling at the transition temperatures are presented. From the table it is clear that the regime transition temperature decreases with an increase in PMA concentration for all the three PVF₂ fractions, but the supercooling required for the regime transition is approximately the same for all the blends ($\Delta T = 36 \pm 3^\circ$). This conforms with the

kinetic nucleation theory of regime transition^{12,34}. However, for KYA and KYD blends there is a slight tendency in the increase of supercooling with increasing PMA concentration for the same regime transition.

The surface energy values obtained from the slopes of the straight lines of Figures 8–10 are presented in Table 3. In this table the standard deviation of the $\sigma\sigma_e$ values are also presented. However, the deviation is larger for regime II than that for regime III, probably because of less data in the lines representing regime II than that of regime III. From the table it is clear that $\sigma\sigma_e$ values calculated in different regimes are not exactly equal except in a few cases. The cause of such anomaly is due to the fact that the ratio of the measured slopes of III to II regimes is not exactly equal to the theoretical value of 2^{12,34}. The cause is as yet uncertain. However, for comparison of the $\sigma\sigma_e$ value one can choose the values for a particular regime and it is clear from the table that the $\sigma\sigma_e$ value gradually decreases with increasing PMA concentration in each case for all the regimes. To explain the cause of the gradual decrease of the $\sigma\sigma_e$ value the individual surface energy values will now be discussed. The end surface free energy σ_e is intramolecular in origin¹², though under specific circumstances it can exhibit variable values, particularly in the presence of a small molecular diluent³⁸. In the presence of a polymeric diluent, the variation of σ_e is not yet reported. A difference between the effect of polymeric diluent and monomeric diluent on the crystallization behaviour of a crystalline polymer is that a monomeric diluent can penetrate into the fold interface^{39,40} while a polymeric diluent is completely rejected from the interface^{41–44}. Thus, a polymeric diluent is expected to remain neutral on the chain folding process and so σ_e will be independent of blend composition¹⁵. Therefore, the observed variation of $\sigma\sigma_e$ with blend composition is expected to be due to the decrease of the σ value. The σ_e value can be measured from both thermodynamic and kinetic points of view¹², and in the literature there are various σ_e values reported for PVF₂. Nakagawa and Ishida²⁶ found for σ_e a value of 146 erg cm⁻² from the slope of the melting point versus reciprocal lamellar thickness plot. In the kinetic method Wang and Nishi¹ determined the value of σ_e to be 47.5 erg cm⁻² and Mancarella and Martuscelli²⁰ reported two values of σ_e , e.g. 65 and 239 erg cm⁻². Since we are dealing with the $\sigma\sigma_e$ values obtained by the kinetic method we should choose a value of σ_e from the kinetic methods. Of the three values

Table 2 Break points in regime transition of PVF₂ fractions and their blends with PMA

System	w_{PMA}	Transition temp. (°C)	Supercooling (ΔT)
KFE	0.0	162	44
	0.12	162	38
	0.25	156	39
	0.39	152	38
	0.53	150	37
KYA	0.00	157	31
	0.11	154	31
	0.26	150	33
	0.40	146	36
	0.51	144	38
KYD	0.00	146	30
	0.09	144	31
	0.25	140	34
	0.41	136	37
	0.52	132	40

Table 3 Surface energies and chain extension factor of PVF₂ in its blend with poly(methyl acrylate)

Polymer	w_{PMA}	Regime I		Regime II			Regime III		
		$\sigma\sigma_e \pm 50$ erg ² cm ⁴	$\sigma \pm 0.3$ erg cm ²	$\sigma\sigma_e \pm 60$ erg ² cm ⁴	$\sigma \pm 0.9$ erg cm ²	$\alpha \pm 0.07$	$\sigma\sigma_e \pm 30$ erg ² cm ⁴	$\sigma \pm 0.5$ erg cm ²	$\alpha \pm 0.04$
KFE	0.0	816	12.5	816	12.5	1.00	—	—	—
	0.12			960	14.7	0.92	912	14.0	—
	0.25			819	12.6	1.00	699	10.7	—
	0.39			489	7.5	1.29	630	9.7	—
	0.53			489	7.5	1.29	522	8.0	—
KYA	0.0			903	13.9	1.00	666	10.2	1.00
	0.11			807	12.4	1.06	606	9.3	1.05
	0.26			711	10.9	1.13	564	8.7	1.09
	0.40			856	13.2	1.03	655	10.1	1.01
	0.51			856	13.2	1.03	594	9.1	1.06
KYD	0.0			885	13.6	1.00	573	8.8	1.00
	0.09			909	13.9	0.99	576	8.8	1.00
	0.25			612	9.4	1.2	420	6.4	1.17
	0.41			564	8.6	1.25	444	6.8	1.13
	0.52			456	7.0	1.39	456	7.0	1.12

reported by this method we found the 65 erg cm^{-2} value is justified since the T_m^0 used⁴⁵ to calculate $\sigma\sigma_e$ for the polymer (KY-301 defect = 5.7%) has been found to be accurate²². Taking this value of σ_e and assuming it is invariant, σ values were measured and are reported in the table. The value of σ calculated from the theoretical expression¹² $\sigma = 0.1(\Delta H_f)(ab)^{1/2} = 9.76 \text{ erg cm}^{-2}$ for PVF₂. As shown from the table, the measured σ values are close to the calculated value and are comparable with those of other straight chain polymers¹².

It is apparent from Table 3 that there is a tendency for a decrease of σ values with increasing PMA concentration in the blend for both the regimes of crystallization. For the blends, the α values were calculated using equation (4) and are also reported in the table. For almost cases α is greater than unity, though no definite trend with blend composition or with H-H defect content is observed. This indicates that in the melt due to blending with PMA, chain extension of PVF₂ occurs. However, no quantitative analysis of the chain extension factor can be given from these data because they are not in exact agreement with the interaction parameter values²⁷ which increase with PMA content and also with H-H defect content of PVF₂ in the blend. This indicates that σ is a complex parameter and apart from its absolute dependency on the thermodynamic property of the melt the structure of the crystal produced from the blend is also playing a specific role¹⁵.

It is pertinent now to discuss the widening of the isothermal temperature range (TR) for the same time period of crystallization (Figure 5) and also the change of regime from I \rightarrow II for pure KFE PVF₂ from II \rightarrow III in its blends. According to a recent attempt of Hoffman *et al.*¹³ to relate σ with the polymer chain structure it has been postulated that the activated state of crystallization process is the formation of a straightened portion of the chain (length = initial lamellar thickness) localized under the influence of crystal surface prior to crystallographic attachment. This 'poised' section of the molecule in a subsequent fast step attaches crystallographically to the substrate. As may be seen from Table 3, the PVF₂ chain becomes extended in the melt of the blend than in pure PVF₂ and consequently the activation energy of the nucleation process in the blend will be smaller. Thus in the blend the nucleation will be faster than that in the pure melt*. But the growth of the nuclei in the blend is, of course, slower than that in the pure PVF₂ melt because it requires the depletion of the amorphous polymer. These two different effects make the isothermal crystallization range wider when increasing the amorphous content of the blend. Also this is the reason why in the KFE PVF₂/PMA blends, no regime I crystallization was seen as observed in the pure KFE PVF₂ fraction. In regime I a single nucleus completes the substrate but since nucleation event in the blend is easier than the growth process, then at the same supercooling there is always more than one nucleus completing the substrate, causing regime II crystallization. Therefore, the extension of the PVF₂ chain in the melt of the blend is the cause of widening of the isothermal temperature range for the same

time period of crystallization and also is the probable cause for the absence of regime I crystallization in any of the PVF₂/PMA blends studied here.

CONCLUSION

From this study we can conclude that at a particular temperature the crystallization rate decreases with an increase in H-H defect content of PVF₂ samples but at a particular supercooling the crystallization rate increases with an increase in H-H defect content. In the case of PVF₂/PMA blends a similar conclusion can be drawn, particularly at low PMA concentration in the blend. H-H defects in PVF₂ have a significant influence on the regime transition. The lower H-H defect (3.75%) PVF₂ fractions exhibit I \rightarrow II regime break while the higher H-H defect (5.0%) fractions exhibit II \rightarrow III regime break within the same time scale (1–3 decades) of crystallization. The $\sigma\sigma_e$ values calculated from the kinetic results decrease with increase in PMA concentration for both the regimes of crystallization (regime II and III) and the cause has been attributed to the decrease of the σ value with the blend composition. The chain extension factor (α), calculated from the ratio of σ values of the blends and of the pure polymer, have values greater than unity, indicating that the PVF₂ chain becomes extended when blended with PMA. This extension of the chain probably causes a widening of the isothermal temperature range for crystallization of the blends with increasing PMA concentration and also causes the absence of regime I crystallization of PVF₂ in the blends.

ACKNOWLEDGEMENTS

We gratefully acknowledge C.S.I.R., New Delhi (grant no. 4(112)/91 EMR-11) for financial assistance.

REFERENCES

1. Wang, T. T. and Nishi, T., *Macromolecules*, 1977, **10**, 421.
2. Ong, C. J. and Price, F. P., *J. Polym. Sci., Polym. Symp.*, 1978, **63**, 59.
3. Saito, H., Okada, T., Hamane, T. and Inoue, T., *Macromolecules*, 1991, **24**, 4446.
4. Briber, R. M. and Khoury, F., *Polymer*, 1987, **28**, 38.
5. Alfonso, G. C. and Russel, T. P., *Macromolecules*, 1986, **19**, 1143.
6. Keith, H. D. and Padden, F. J. Jr., *J. Appl. Phys.* 1964, **35**, 1270; 1964, **35**, 1286.
7. Lauritzen, J. I. Jr. and Hoffman, J. D., *J. Appl. Phys.*, 1973, **44**, 4340.
8. Boon, J. and Azcue, J. M., *J. Polym. Sci., Polym. Phys. Ed.*, 1968, **6**, 885.
9. Flory, P. J., *J. Chem. Phys.*, 1949, **17**, 223.
10. Mandelkern, L., *J. Appl. Phys.*, 1955, **26**, 443.
11. Mandelkern, L., *Crystallization of polymers*. McGraw-Hill, New York, 1964, p. 273.
12. Hoffman, J. D., Davis, G. T. and Lauritzen, J. I., Jr. In: *Treatise on Solid State Chemistry*, Vol.3, ed. N. B. Hannay. Plenum Press, New York, 1975.
13. Hoffman, J. D., Miller, R. L., Marand, H. and Roitman, D. B., *Macromolecules*, 1992, **25**, 2221.
14. Flory, P. J. *Statistical Mechanics of Chain Molecules*. Interscience, New York, 1969, p. 11.
15. Huang, J., Prasad, A. and Marand, H., *Polymer*, 1994, **35**, 1896.
16. Lovinger, A. J. In: *Developments in crystalline polymer I*, ed. D. C. Bassett. Applied Science Publishers, London, 1981 p. 195.
17. Majumdar, R. N. and Harwood, H. J. In: *Applied polymer analysis and characterization*, ed. J. Mitchel, Jr. Hanser Pub., New York, 1987, p. 423.
18. Gianotti, G., Cappizzi, A. and Zamboni, V., *Chim. Industr.*, 1973, **55**, 501.

* According to equation (1) the nucleation rate should be lower in the diluted system, but this equation was derived considering only the probability of selecting the crystalline sequences from the mixture⁸. However, in the mixing process of the PVF₂/PMA system there is some favourable interaction²⁷ which causes the chain extension. Therefore, the enhancement of nucleation is due to interactional force which was not counted in deriving equation (1).

19. Nakamura, S., Sasaki, T., Funamoto, J. and Matsuzaki, K., *Die Makromol. Chem.*, 1975, **176**, 3471.
20. Mancarella, C. and Martusceli, E., *Polymer*, 1977, **18**, 1240.
21. Nandi, A. K. and Mandelkern, L. In preparation.
22. Nandi, A. K. and Mandelkern, L., *J. Polym. Sci., Polym. Phys. Ed.*, 1991, **29**, 1287.
23. Maiti, P., Chatterjee, J., Rana, D. and Nandi, A. K., *Polymer*, 1993, **34**, 4273.
24. Weinhold, S., Litt, M. H. and Lando, J. B., *J. Appl. Phys.*, 1980, **51**, 5154.
25. Marand, H. L., Stein, R. S. and Stack, G. M., *J. Polym. Sci., Polym. Phys., Ed.*, 1988, **26**, 1361.
26. Nakagawa, K. and Ishida, Y., *J. Polym. Sci., Polym. Phys. Ed.*, 1973, **11**, 2153.
27. Maiti, P. and Nandi, A. K., *Macromolecules*, 1995, **28**, 8511.
28. Morra, B. S. and Stein, R. S., *J. Polym. Sci., Polym. Phys. Ed.*, 1982, **20**, 2243.
29. Fox, T.G., *Bull Am. Phys. Soc.*, 1950, **1**, 123.
30. Eds. Brandrup, J. and Immergut, E. H. *Polymer Handbook*, 2nd edn. Wiley, New York, 1975.
31. Wood, L.A., *J. Polym. Sci.*, 1958, **28**, 319.
32. Flory, P. J., *Trans Faraday Soc.*, 1955, **51**, 848.
33. Maiti, P. and Nandi, A. K., unpublished work.
34. Hoffman, J. D., *Polymer*, 1983, **24**, 3.
35. Lovinger, A. J., *J. Polym. Sci., Polym. Phys. Ed.*, 1980, **18**, 793.
36. Miller, R. L. and Welch, G. J. In: *Flow Induced Crystallization in Polymer Systems*, ed. R. L. Miller. Gordon and Breach, New York, 1979.
37. Tomura, H., Saito, H. and Inoue, T., *Macromolecules*, 1992, **25**, 1611.
38. Nakajima, A., Hamada, F., Hayashi, S. and Sumida, T., *Kolloid Z. Z. Polym.*, 1968, **22**, 10.
39. Udagawa, Y. and Keller, A., *J. Polym. Sci., Polym. Phys. ed.*, 1971, **9**, 437.
40. Ergoz, E. and Mandelkern, L., *J. Polym. Sci., Polym. Lett. Edn.*, 1972, **10**, 631.
41. Hahn, B., Wendorff, J. and Yoon, D. Y., *Macromolecules*, 1985, **18**, 718.
42. Hahn, B., Herrmann-Schönherr, O. and Wendorff, J. H., *Polymer*, 1987, **28**, 201.
43. Russel, T. P., Ito, H. and Wignall, G. D., *Macromolecules*, 1988, **21**, 1703.
44. Yoon, D. Y., Ando, Y., Rojstaczer, S., Kumar, S. K. and Alfonso, G. C., *Makromol Chem. Macromol Symp.*, 1991, **50**, 183.
45. Welch, G. J. and Miller, R. L., *J. Polym. Sci., Polym. Phys. Edn.*, 1976, **14**, 1683.